ACI STRUCTURAL JOURNAL TECHNICAL PAPER

Title no. 102-S51

Seismic Design Guidelines for Squat Composite-Jacketed Circular and Rectangular Reinforced Concrete Bridge Columns

by Hussein M. Elsanadedy and Medhat A. Haroun

An object-oriented computer code, based on a moment-curvature analysis with inclusion of fiber-reinforced polymer-confined concrete models, was developed to predict the seismic performance of reinforced concrete squat bridge columns. The study involved seismic assessment of as-built shear-deficient columns in addition to performance prediction of ductile composite-jacketed columns. For as-built columns, the code assessed the accuracy of several shear strength models using experimental data of 65 shear-deficient columns. For composite-jacketed columns, the developed software was calibrated through a parametric study of two displacement models and six different concrete confinement models. Subsequently, a methodology for the seismic design of shear-deficient columns upgraded with composite-material jackets was devised.

Keywords: bridge; column; reinforced concrete; seismic.

INTRODUCTION

One of the major problems associated with seismic performance of older reinforced concrete (RC) bridges is brittle shear failure of squat columns. Such short and relatively stiff members tend to attract a greater portion of the seismic input to the bridge and require the generation of large seismic shear forces to develop the moment capacity of column section. Estimation of flexural strength based on elastic methods, along with much less conservative shear strength provisions during the 1950s and 1960s, frequently resulted in the actual shear strength of as-built bridge columns being less than the flexural capacity. Generally, the transverse reinforcing steel was inadequately anchored in the cover concrete, which can be expected to spall off under cyclic loading; therefore, the problem was compounded. Hence, shear failure is likely in such columns, accompanied not only by rapid strength, stiffness, and physical degradation, but also by poor energy dissipation characteristics. This has been evidenced by brittle shear failure of bridge columns in past California earthquakes.

To upgrade bridge columns with insufficient shear reinforcement, several retrofit measures were developed by researchers and practicing engineers. Composite materials are recently recognized as reliable alternatives to steel jacketing. Advantages of composite retrofit systems include light weight, high strength or stiffness-to-weight ratios, corrosion resistance, and, in particular, ease of installation. Moreover, composite-material jackets will not affect the lateral stiffness of columns, and hence will not alter bridge dynamic characteristics. A fundamental objective of the current research is to establish practical design criteria for columns retrofitted by composite-material jackets. The retrofit design philosophy of squat bridge columns is fully detailed in this paper.

RESEARCH SIGNIFICANCE

Lack of shear reinforcement in older squat RC bridge columns caused brittle shear failures during past earthquakes. This research provides effective and economical procedures for seismic retrofit and repair of shear-deficient columns. Furthermore, utilization of new materials such as fiber composites provides an insight into alternative materials for various applications in civil engineering.

ANALYTICAL MODELING

To predict the performance of RC squat columns, an object-oriented computer code was developed. The program is based on moment-curvature analysis of the column section with inclusion of concrete confinement models and shear strength models. Its main purpose is to provide bridge engineers with a simplified tool to assess the capacity of squat columns with an allowance to try different types of composite-jacket retrofit. The program reads column data (dimensions, reinforcement details, concrete strength, yield stress of steel, axial load, and mechanical properties of fiber-reinforced polymer [FRP] jacket) via an input text file. Upon running the program, it creates an output text file containing analysis results such as moment-curvature calculations, load-displacement envelopes, and shear strength envelopes.

In defining the constitutive properties, concrete is of key concern. For as-built columns, concrete is considered unconfined, and Mander's equations for unconfined concrete[1] were used. For retrofitted columns, however, six different confined concrete models were employed. The first model was developed by Mander, Priestley, and Park;[1] it was successfully applied to both circular and rectangular steel-jacketed columns. The second was proposed by Samaan, Mirmiran, and Shahawy[2] specifically for circular composite-jacketed columns. The third model, developed by Hosotani, Kawashima, and Hoshikuma,[3] is applicable to both circular and rectangular composite-jacketed columns. The fourth model was suggested by Hoppel et al.[4] for circular columns only. Toutanji[5] and Spoelstra and Monti,[6] respectively, developed two other models limited to circular FRP-jacketed columns. A model of the stress-strain properties of steel reinforcement was also incorporated into the code. This model was divided into three major zones: a linear portion up to yield point, a yield plateau region, and a parabolic

ACI Structural Journal, V. 102, No. 4, July-August 2005.
MS No. 03-110 received March 12, 2003, and reviewed under Institute publication policies. Pertinent discussion including author's closure, if any, will be published in the May-June 2006 *ACI Structural Journal* if the discussion is received by January 1, 2006.

Hussein M. Elsanadedy *is an assistant professor of civil engineering at Helwan University, Cairo, Egypt. He received his BSc and MSc from Helwan University, and his PhD in structural engineering from the University of California, Irvine, Calif., in 2002. His research interests include seismic retrofit and rehabilitation of concrete structures using fiber composites and failure analysis, and damage assessment of buildings and bridges.*

Medhat A. Haroun *is Dean and AGIP Professor, School of Sciences and Engineering, American University in Cairo, Cairo, Egypt, and Professor Emeritus, Department of Civil and Environmental Engineering, University of California, Irvine, Calif. His research interests include theoretical and experimental modeling of the seismic behavior of structural systems such as liquid storage tanks, bridge structures, and buildings.*

strain-hardening curve. Perfect bond was assumed between longitudinal steel and the surrounding concrete.

The column analysis was handled by a laminar approach. The moment-curvature relationship was determined by equilibrium of internal axial forces on the column section through use of convergence criteria. To compute the top lateral displacement of the column, two displacement models due to Kowalsky, Priestley, and Seible[7] and Wehbe, Saiidi, and Sanders[8] were used; shear deformation is incorporated in both models. In addition, two sets of shear strength provisions were employed; for the first set, concrete contribution to shear strength degrades as column displacement ductility increases. Such an approach is used in the UCSD shear strength model,[9] Caltrans model,[10] UCB shear strength model,[11] and Architectural Institute of Japan (AIJ) seismic design guidelines.[12] The second set includes shear strength provisions at which concrete contribution to shear strength does not depend on the displacement ductility, such as ACI 318-95 provisions,[13] Joint ACI-ASCE Committee 426 proposals,[14] and ATC-32 provisions.[15] Full details of all models, in addition to the numerical procedure, are reported elsewhere.[16]

MODEL CALIBRATION

Shear-deficient columns

The computer code for the prediction of performance of shear-deficient columns was calibrated using a large experimental database collected from the literature. The database included columns tested under different parameters such as displacement ductility factor $\mu_{\Delta u}$, column aspect ratio M/VD, end conditions (single- or double-bending configurations), axial load ratio $P/f_c'A_g$, and transverse steel ratio ρ_s. The total population included 47 circular and 18 rectangular columns identified as having failure strongly influenced by shear. Tests on circular columns were conducted by Haroun et al.;[17] Navalpakkam;[18] Verma, Priestley, and Seible;[19] Priestley, Seible, and Benzoni;[20] Benzoni et al.;[21] Ohtaki, Benzoni, and Priestley;[22] Ang;[23] Wong, Paulay, and Priestley;[24] Xiao, Wu, and Martin;[25] and Iwasaki et al.[26] Rectangular samples were tested by Haroun et al.;[17] Xiao, Priestley, and Seible;[27] Jirsa and Woodward;[28] Bett, Klingner, and Jirsa;[29] and Okamoto et al.[30] Table 1 and 2 show the parameters of the circular and rectangular columns, respectively. It should be noted that in the designation of test samples, the letters C and R denote circular and rectangular columns, respectively, the letter S denotes shear testing, and the letter A stands for as-built columns.

A statistical study was carried out on the experimental-to-theoretical (tested-to-predicted) shear strength ratio $V_{u\text{-}exp}/V_{u\text{-}th}$, and the statistical parameters are displayed in Table 3. These are the mean m to measure the center of distribution, maximum value, minimum value, standard deviation σ, and coefficient of variation (COV) to measure the dispersion of

Table 1—Experimental database for circular shear-deficient columns

Sample	Bending	Aspect ratio	Axial load ratio	Transverse steel ratio	$V_{u\text{-}exp}$, kN	$\mu_{\Delta u\text{-}exp}$
CS-A1[17]	Double	2	0.06	0.00176	426.6	1.37
CS-A2[18]	Double	2	0.05	0.00126	326.0	1.00
CS-A3[19]	Double	2	0.06	0.00173	573.8	2.50
CS-A4[19]	Double	2	0.18	0.00173	733.9	3.00
CS-A5[19]	Double	2	0.06	0.00173	613.8	1.00
CS-A6[19]	Double	1.5	0.06	0.00173	791.7	1.00
CS-A7[20]	Double	1.5	0.06	0.00173	587.4	3.50
CS-A8[21]	Double	2	0.35	0.00307	492.6	1.50
CS-A9[22]	Single	2	0	0.00099	310.4	1.30
CS-A10[23]	Single	2	0	0.00580	320.0	2.50
CS-A11[23]	Single	2	0	0.00580	228.0	4.00
CS-A12[23]	Single	2.5	0	0.00580	298.0	4.00
CS-A13[23]	Single	2	0	0.00478	295.0	1.40
CS-A14[23]	Single	2	0	0.00872	340.0	2.40
CS-A15[23]	Single	1.5	0	0.00580	390.0	1.30
CS-A16[23]	Single	2	0	0.00434	280.0	1.60
CS-A17[23]	Single	2	0.20	0.01160	475.0	4.00
CS-A18[23]	Single	2	0.20	0.1200	450.0	4.00
CS-A19[23]	Single	2	0.20	0.00580	404.0	2.50
CS-A20[23]	Single	1.5	0.10	0.01160	527.0	3.00
CS-A21[23]	Single	2	0.10	0.01160	443.0	4.00
CS-A22[23]	Single	2	0	0.00580	311.0	2.00
CS-A23[23]	Single	2	0	0.00580	230.0	4.00
CS-A24[23]	Single	2	0.10	0.00580	379.0	1.50
CS-A25[23]	Single	2.5	0.10	0.00580	329.0	2.00
CS-A26[23]	Single	1.5	0.10	0.00580	507.0	1.40
CS-A27[23]	Single	1.5	0.10	0.00434	436.0	1.30
CS-A28[23]	Single	1.75	0.18	0.00434	487.0	1.50
CS-A29[23]	Single	2	0	0.00434	258	1.10
CS-A30[23]	Single	2	0	0.00359	280.0	1.50
CS-A31[23]	Single	2	0	0.00899	339.0	2.00
CS-A32[23]	Single	2	0	0.00718	338.0	4.00
CS-A33[24]	Single	2	0.39	0.00535	514.8	2.00
CS-A34[24]	Single	2	0	0.00434	320.1	1.25
CS-A35[24]	Single	2	0	0.00695	349.8	2.00
CS-A36[24]	Single	2	0	0.01160	359.7	3.00
CS-A37[24]	Single	2	0.19	0.00580	458.3	2.00
CS-A38[24]	Single	2	0.19	0.01160	498.5	3.00
CS-A39[24]	Single	2	0.39	0.00872	425.6	3.00
CS-A40[24]	Single	2	0.39	0.01214	545.7	4.0
CS-A41[24]	Single	2	0	0.01160	339.9	2.00
CS-A42[24]	Single	2	0	0.02252	323.4	3.00
CS-A43[24]	Single	2	0.19	0.01160	478.4	3.00
CS-A44[24]	Single	2	0.19	0.01317	432.7	3.00
CS-A45[24]	Single	2	0.19	0.01160	518.7	4.00
CS-A46[25]	Double	1.5	0.06	0.00147	580.0	2.50
CS-A47[26]	Single	1.77	0	0.00218	419.0	3.47

Table 2—Experimental database for rectangular shear-deficient columns

Sample	Bending	Aspect ratio	Axial load ratio	Transverse steel ratio	$V_{u\text{-}exp}$, kN	$\mu_{\Delta u\text{-}exp}$
RS-A1[17]	Double	2	0.07	0.00121	405.7	0.80
RS-A2[27]	Double	2	0.05	0.00138	565.8	3.00
RS-A3[27]	Double	2	0.06	0.00138	627.2	1.30
RS-A4[27]	Double	1.5	0.06	0.00138	747.3	0.80
RS-A5[28]	Double	1.5	0	0.00392	244.6	2.50
RS-A6[28]	Double	1.5	0.16	0.00392	302.5	1.50
RS-A7[28]	Double	1.5	0	0.00895	280.2	3.00
RS-A8[28]	Double	1.5	0.15	0.00895	355.8	2.00
RS-A9[28]	Double	1.5	0.14	0.00575	360.3	2.00
RS-A10[28]	Double	1.5	0.18	0.00392	289.1	2.00
RS-A11[28]	Double	1.5	0.14	0.00252	298.0	1.00
RS-A12[28]	Double	1.5	0.14	0.00084	324.7	1.00
RS-A13[29]	Double	1.5	0.10	0.00215	209.1	—
RS-A14[30]	Single	2.5	0	0.00310	121.6	—
RS-A15[26]	Single	3.5	0	0.00111	237.5	3.28
RS-A16[26]	Single	2	0	0.00111	383.4	1.87
RS-A17[26]	Single	3.5	0	0.00111	241.5	3.64
RS-A18[26]	Single	2	0	0.00111	419.0	1.66

distribution. It is concluded that the UCSD model provides a much better correlation with the experimental data than all of the other models. This model has a mean value of tested-to-predicted shear strength of 1.065, with the least scatter as indicated in its COV of 10.08%. For other shear models, the mean and COV are less accurate, particularly the ATC-32 approach that has a mean value of tested-to-predicted shear strength of 2.074 and a COV of 29.68%. Table 4 displays statistical lower bounds of the ratio of tested-to-predicted shear strength in terms of $m - \sigma$, $m - 2\sigma$, and $m - 3\sigma$. These, respectively, provide 84.13, 97.72, and 99.87% probabilities that the indicated values are exceeded. The $m - 2\sigma$ value is higher for the UCSD model than for the other approaches despite the much lower mean value; this implies lower probability of severe overprediction of shear strength in extreme cases.

Due to its brittle nature, shear is regarded as a mode of failure that should be avoided in RC bridge column design. Therefore, the proposed design knockdown factor for shear strength calculations is based on statistical lower bounds of the ratio of tested-to-predicted shear strength in the terms of $m - 2\sigma$. Accordingly from Table 4, applying a 0.85 factor to the shear strength predicted by the UCSD model provides a reasonable design value for the shear strength. Such a decrease in the strength predicted by the UCSD model would result in a design approach that still has a lower mean strength ratio than other design equations given by Caltrans,[10] ACI 318-95,[13] Joint ACI-ASCE Committee 426,[14] and ATC-32[15] (and would hence be more economical), while providing a better protection against shear failure for the low end of the experimental database.

Composite-jacketed columns

In addition to as-built shear-deficient columns, the developed computer code was employed to evaluate the seismic performance of squat composite-jacketed columns. An

Table 3—Statistical analysis for all data of shear-deficient columns

Model	$(V_{u\text{-}exp}/V_{u\text{-}th})$						
	m	σ	COV, %	Maximum value	Minimum value	No. of tested samples	No. of shear failure predictions
UCSD[9]	1.065	0.107	10.08	1.261	0.794	65	65
Caltrans[10]	1.260	0.238	18.89	1.846	0.808	65	65
UCB[11]	1.090	0.140	12.88	1.465	0.790	65	61
AIJ[12]	1.139	0.221	19.37	1.769	0.843	65	59
ACI 318-95 approximate[13]	1.385	0.331	23.90	2.520	0.809	65	59
ACI 318-95 refined[13]	1.462	0.375	25.65	2.775	0.798	65	60
ACI-ASCE 426 approximate[14]	1.320	0.292	22.16	2.205	0.788	65	49
ACI-ASCE 426 refined[14]	1.304	0.264	20.26	2.108	0.788	65	56
ATC-32[15]	2.074	0.616	29.68	3.711	0.837	65	65

Table 4—Statistical lower bounds for all data of shear-deficient columns

Model	$(V_{u\text{-}exp}/V_{u\text{-}th})$			
	$m - \sigma$	$m - 2\sigma$	$m - 3\sigma$	Design value
UCSD[9]	0.958	0.850	0.743	0.85
Caltrans[10]	1.022	0.784	0.546	—
UCB[11]	0.950	0.809	0.669	—
AIJ[12]	0.918	0.698	0.477	—
ACI 318-95 approximate[13]	1.054	0.723	0.392	—
ACI 318-95 refined[13]	1.087	0.712	0.337	—
ACI-ASCE 426 approximate[14]	1.027	0.735	0.443	—
ACI-ASCE 426 refined[14]	1.040	0.776	0.511	—
ATC-32[15]	1.458	0.843	0.227	—

experimental database of circular and rectangular composite-jacketed columns was collected from the literature, and the properties of these samples are listed in Table 5 and 6. Further to aforementioned definitions, the letters R and P stand for retrofitted and repaired columns, respectively. Tests on circular composite-jacketed columns were carried out by Haroun et al.;[17] Ohtaki, Benzoni, and Priestley;[22] Seible et al.;[31] and Gallagher.[32] The database for rectangular composite-jacketed columns, however, was only from tests by Haroun et al.[17]

For circular columns, ratios of experimental-to-theoretical maximum lateral load $V_{u\text{-}exp}/V_{u\text{-}th}$, ultimate displacement $\Delta_{u\text{-}exp}/\Delta_{u\text{-}th}$, and ultimate ductility $\mu_{\Delta u\text{-}exp}/\mu_{\Delta u\text{-}th}$ were calculated for the different displacement and confinement models. It is concluded that best fit to the experimental data was provided by Wehbe's model for displacement calculation along with Hosotani, Kawashima, and Hoshikuma's model for FRP-confined concrete. This is further demonstrated by comparing these values for Sample CS-R1 as shown in Fig. 1. Based on the best-fit models, theoretical load-displacement curves were generated and compared with the experimental results as displayed in Fig. 2(a) and (b) for Samples CS-R1 and CS-P2, respectively.

As stated previously, Mander, Priestley, and Park's and Hosotani, Kawashima, and Hoshikuma's confinement

Table 5—Details and dimensions of squat composite-jacketed columns

Sample	Column height, m	Bending	Column dimensions, mm	Axial load, kN	Concrete cover,* mm	Main steel
CS-R1[17]	2.44	Double	D = 610	645	25	20 No. 6 (d_{bl} = 19 mm) G40
CS-R2[17]	2.44	Double	D = 610	645	25	20 No. 6 (d_{bl} = 19 mm) G40
CS-R3[17]	2.44	Double	D = 610	645	25	26 No. 6 (d_{bl} = 19 mm) G60
CS-R4[17]	2.44	Double	D = 610	645	25	20 No. 6 (d_{bl} = 19 mm) G60
CS-R5[31]	1.83	Double	D = 610	1779	38	10 No. 6 (d_{bl} = 19 mm) G40
CF-P1[17]	2.44	Double	D = 610	645	25	20 No. 6 (d_{bl} = 19 mm) G60
CS-P2[22]	3.66	Single	D = 1829	0.0	64	24 No. 14 (d_{bl} = 43 mm) G60
CS-P3[22]	2.44	Double	D = 610	592	19	26 No. 6 (d_{bl} = 19 mm) G60
RS-R1[17]	2.44	Double	457 x 610	676	25	20 No. 6 (d_{bl} = 19 mm) G40
RS-R2[17]	2.44	Double	457 x 610	676	25	20 No. 6 (d_{bl} = 19 mm) G40
RS-R3[17]	2.44	Double	457 x 610	676	25	20 No. 6 (d_{bl} = 19 mm) G40
RS-R4[17]	2.44	Double	457 x 610	676	25	20 No. 6 (d_{bl} = 19 mm) G40
RS-R5[17]	2.44	Double	457 x 610	676	25	20 No. 6 (d_{bl} = 19 mm) G40
RS-R6[17]	2.44	Double	457 x 610	676	25	20 No. 6 (d_{bl} = 19 mm) G40

*Measured to main steel.
Notes: d_{bl} = diameter of longitudinal bar; G40 = Grade 40 steel (nominal yield strength = 276 MPa); and G60 = Grade 60 steel (nominal yield strength = 414 MPa).

Table 6—Material properties of squat composite-jacketed columns

Test sample	Concrete strength, MPa	Yield stress of main steel, MPa	Composite jacket properties			
			Type	Thickness within plastic hinge zone, mm	Tensile strength, MPa	Tensile modulus, GPa
CS-R1	40.8	299.1	Carbon/epoxy	0.7	4168	231.5
CS-R2	39.2	299.1	Carbon/epoxy	0.7	4430	230.1
CS-R3	34.2	480.7	E-glass/epoxy	10.3	424	18.5
CS-R4	37.6	480.7	Carbon/epoxy	1.2	1245	103.8
CS-R5	37.1	292.8	Carbon/epoxy	4.3	1391.8	111.6
CS-P1	35.7	480.7	Carbon/epoxy	2.3	1245	103.8
CS-P2	29.6	508.5	E-glass/epoxy	9.8	425.1	23.4
CS-P3	39.3	485.7	Carbon/epoxy	4.1	1274.7	115.1
RS-R1	38.1	299.1	Carbon/epoxy	1.0	4382	226.0
RS-R2	39.3	299.1	Carbon/epoxy	1.0	4430	230.1
RS-R3	44.0	299.1	Carbon/epoxy	1.0	4168	231.5
RS-R4	44.0	299.1	E-glass/vinylester	7.6	744	36.5
RS-R5	44.0	299.1	Carbon/epoxy	5.2	937	63.0
RS-R6	42.6	299.1	E-glass/polyester	7.6	641	36.4

models are the only models applicable to rectangular columns. A similar parametric study was conducted for rectangular retrofitted samples and showed that Kowalsky, Priestley, and Seible's displacement model along with Hosotani, Kawashima, and Hoshikuma's model for FRP-confined concrete provide the best fit to the experimental results. This is demonstrated in Fig. 3 for Sample RS-R2, and further validated in Fig. 4(a) and (b) for Samples RS-R5 and RS-R6, respectively.

In addition to performance prediction, a statistical study was carried out on $V_{u\text{-}exp}/V_{u\text{-}th}$ and $\mu_{\Delta u\text{-}exp}/\mu_{\Delta u\text{-}th}$ ratios for composite-jacketed columns. Because the experimental lateral force-displacement relationship for circular repaired columns is essentially the same as that for the corresponding

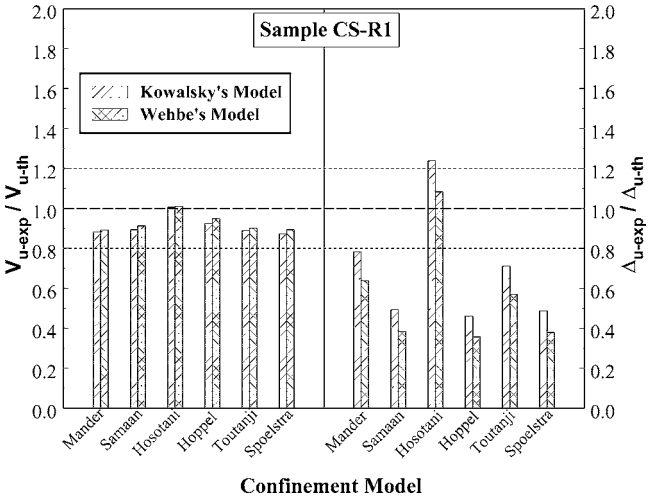

Fig. 1—Experimental and theoretical comparison of flexural response of Sample CS-R1.

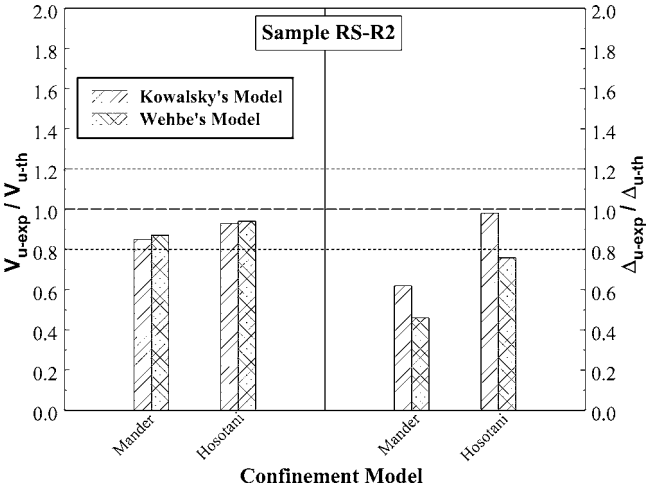

Fig. 3—Experimental and theoretical comparison of flexural response of Sample RS-R2.

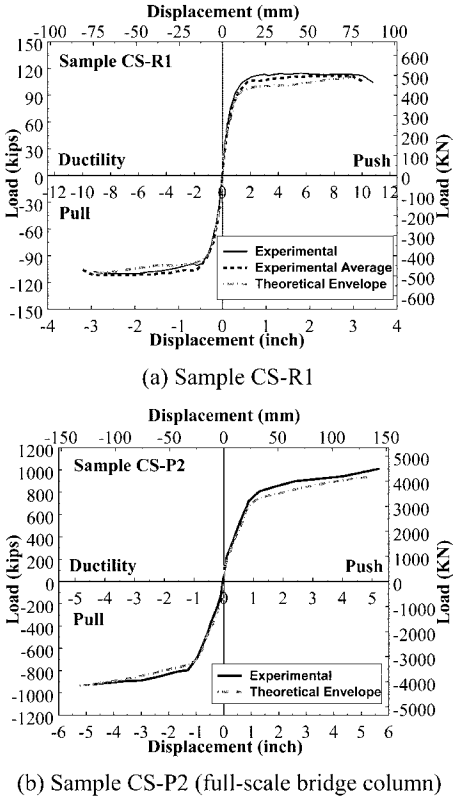

Fig. 2—Comparison between load-displacement envelopes for circular fiber-reinforced polymer-jacketed columns.

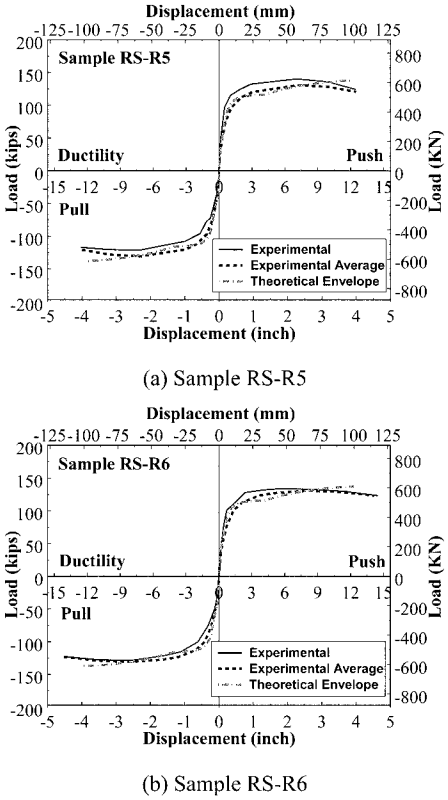

Fig. 4—Comparison between load-displacement envelopes for rectangular fiber-reinforced polymer-jacketed columns.

retrofitted undamaged columns, both retrofitted and repaired circular samples were included in the statistical study. Samples CS-R3 and CS-P1 were excluded from the statistical analysis because they were not confirmed to reach failure in the test. Therefore, the statistical analysis of circular jacketed columns was based on six samples (CS-R1, CS-R2, CS-R4, CS-R5, CS-P2, and CS-P3), whereas Samples RS-R1 to RS-R6 were used in the statistical study of rectangular jacketed columns. Statistical parameters of $V_{u\text{-}exp}/V_{u\text{-}th}$ and $\mu_{\Delta u\text{-}exp}/\mu_{\Delta u\text{-}th}$ ratios are listed in Table 7. These values are based on Wehbe, Saiidi, and Sanders' displacement model for circular columns and Kowalsky, Priestley, and Seible's displacement model for rectangular columns. Hosotani, Kawashima, and Hoshikuma's model for FRP-confined concrete provided the best fit to the data of all FRP-jacketed columns.

RETROFIT DESIGN FACTORS

In seismic retrofit of squat bridge columns, selection of design factors should be based on careful understanding of the adopted design methodology. To integrate safety factors in the retrofit approach, the predicted ultimate displacement ductility for the retrofitted bridge column should be first reduced and then compared with the demand value. This is accomplished by a knockdown coefficient based on statistical lower bounds for the $\mu_{\Delta u\text{-}exp}/\mu_{\Delta u\text{-}th}$ ratio. The case of seismic retrofit of bridge columns is very different from gravity load

Table 7—Statistical analysis for squat composite-jacketed columns

Column section	Confinement model	$(V_{u\text{-}exp}/V_{u\text{-}th})$				$(\mu_{\Delta u\text{-}exp}/\mu_{\Delta u\text{-}th})$			
		m	σ	Maximum value	Minimum value	m	σ	Maximum value	Minimum value
Circular	Mander, Priestley, and Park[1]	0.950	0.069	1.075	0.893	0.752	0.081	0.897	0.672
	Samaan, Mirmiran, and Shahawy[2]	0.964	0.107	1.172	0.875	0.467	0.076	0.565	0.376
	Hosotani, Kawashima, and Hoshikuma[3]	1.059	0.055	1.162	1.011	1.119	0.095	1.244	1.024
	Hoppel et al.[4]	0.996	0.120	1.222	0.889	0.433	0.124	0.588	0.277
	Toutanji[5]	0.965	0.092	1.146	0.901	0.610	0.103	0.776	0.458
	Spoelstra and Monti[6]	0.945	0.105	1.153	0.868	0.435	0.042	0.505	0.383
Rectangular	Mander, Priestley, and Park[1]	0.862	0.015	0.881	0.848	0.519	0.049	0.565	0.424
	Hosotani, Kawashima, and Hoshikuma[3]	0.934	0.013	0.951	0.920	0.754	0.070	0.846	0.661

design. In the latter, it is essential that an adequate margin be maintained between strength and applied loads to avoid failure, whereas in the former, having a wide margin between ductility demand and capacity is not that necessary. Therefore, the knockdown factor for the ultimate displacement ductility was based on statistical lower bounds for the $\mu_{\Delta u\text{-}exp}/\mu_{\Delta u\text{-}th}$ ratio in terms of minimum value and $m - \sigma$, rather than $m - 2\sigma$ that was used in case of design for shear strength. Once the composite jacket for the plastic hinge zones is designed for a ductility capacity-demand ratio greater than 1.0, the retrofitted column should be protected against unfavorable brittle modes such as diagonal shear failure within and outside the plastic hinge zones and shear-friction failure at the column base. To achieve this protection, the demand lateral load should correspond to maximum feasible extreme estimates of flexural strength developing at the plastic hinge after column retrofit. Accordingly, the retrofit design factor for maximum lateral load should be based on statistical upper bounds for the $V_{u\text{-}exp}/V_{u\text{-}th}$ ratio in terms of maximum value and $m + \sigma$.

Statistical lower and upper bounds of $V_{u\text{-}exp}/V_{u\text{-}th}$ and $\mu_{\Delta u\text{-}exp}/\mu_{\Delta u\text{-}th}$ ratios are listed in Table 8, along with recommended retrofit design factors. Because of the limited number of test data of squat composite-jacketed columns under lateral cyclic loading, the statistical analysis was only based on six circular and six rectangular columns. This population size is small, and therefore, the derived retrofit design factors should be considered as guidelines only and are possibly subject to further refinement with the availability of a larger experimental database.

MATERIAL PROPERTIES FOR SEISMIC RETROFIT DESIGN

Concrete strength

The most probable concrete strength should be based, wherever possible, on compression tests of representative concrete cores taken from the bridge under consideration (Priestley, Seible, and Calvi[33]). When testing is not feasible, however, the expected concrete strength may be obtained from[33]

$$f'_{ce} = 1.5f'_{c(28)} \geq 34.45 \text{ MPa (5000 psi)} \quad (1)$$

where $f'_{c(28)}$ is the specified 28-day concrete strength. The lower limit in this equation is proposed as supported by inspection of many old bridges in California.

Table 8—Statistical lower and upper bounds for squat composite-jacketed columns

	Circular columns		Rectangular columns	
	$(V_{u\text{-}exp}/V_{u\text{-}th})$	$(\mu_{\Delta u\text{-}exp}/\mu_{\Delta u\text{-}th})$	$(V_{u\text{-}exp}/V_{u\text{-}th})$	$(\mu_{\Delta u\text{-}exp}/\mu_{\Delta u\text{-}th})$
$m - \sigma$	1.00	1.02	0.92	0.68
Minimum value	1.01	1.02	0.92	0.66
$m + \sigma$	1.11	1.21	0.95	0.82
Maximum value	1.16	1.24	0.95	0.85
Design value	1.15	1.00	0.95	0.65

Steel reinforcement

The strength of steel reinforcement (Priestley, Seible, and Calvi[33]) should, where possible, be determined from mill certificates or from representative samples taken from the bridge. In cases where testing is not feasible and mill certificates are not available, the expected yield stress of reinforcing steel f_{ye} may be obtained from[34]

$$f_{ye} = \begin{cases} 336.2 \text{ MPa (48.8 ksi) for Grade 40 steel} \\ 489.2 \text{ MPa (71.0 ksi) for Grade 60 steel} \end{cases} \quad (2)$$

Fiber-reinforced polymer systems

To specify design properties for FRP systems, the average properties are first determined from the manufacturer (supplier). The tensile strength and strain at rupture are required in terms of mean values (f_{ju} and ε_{ju}, respectively) and a standard deviation σ. Whenever possible, environmental reduction factors for tensile modulus, tensile strength, and strain at rupture should be determined from environmental durability tests. The design properties of the FRP system are then determined according to the following proposed procedure:

Stress-strain method—The guaranteed material properties are first attained from

$$f^*_{ju} = f_{ju} - 3\sigma \text{ and } \varepsilon^*_{ju} = \varepsilon_{ju} - 3\sigma \quad (3)$$

It should be noted that the properties calculated in Eq. (3) provide a 99.87% probability that the indicated values are exceeded. Thereafter, the design properties are given by

$$f_{ju(design)} = C_{EF} f_{ju}^{*} \text{ and } \varepsilon_{ju(design)} = C_{E\varepsilon} \varepsilon_{ju}^{*} \quad (4)$$

$$E_{j(design)} = \frac{f_{ju(design)}}{\varepsilon_{ju(design)}} \leq C_{EM} E_j \quad (5)$$

where E_j is the tensile modulus of the FRP system (from the manufacturer); and C_{EF}, $C_{E\varepsilon}$, and C_{EM} are environmental reduction factors for tensile strength, ultimate strain, and tensile modulus, respectively. If Eq. (5) is not satisfied, the stress-modulus method should be employed.

Stress-modulus method—The design properties are computed from

$$E_{ju(design)} = C_{EM} E_j \text{ and } f_{ju(design)} = C_{EF} f_{ju}^{*} \quad (6)$$

$$\varepsilon_{ju(design)} = \frac{f_{ju(design)}}{E_{j(design)}} \leq C_{E\varepsilon} \varepsilon_{fu}^{*} \quad (7)$$

If Eq. (7) is not verified, the strain-modulus method should be used.

Strain-modulus method—The design properties are given by

$$E_{j(design)} = C_{EM} E_j \text{ and } \varepsilon_{ju(design)} = C_{E\varepsilon} \varepsilon_{ju}^{*} \quad (8)$$

$$f_{ju(design)} = E_{j(design)} \varepsilon_{ju(design)} \leq C_{EF} f_{ju}^{*} \quad (9)$$

In this method, Eq. (9) has to be verified.

RETROFIT DESIGN METHODOLOGY

The following procedures are recommended for seismic retrofit of circular and rectangular squat shear-deficient columns using FRP jackets. The retrofit methodology is divided into five major steps. The first step determines the material properties as stated previously, whereas the second assesses the seismic performance of existing column. In the third step, an FRP jacket for plastic hinge confinement is designed. The fourth step includes design of a composite jacket for shear strength enhancement within and outside the plastic hinge regions. The final step checks jacket design to avoid high diagonal compression stress levels in the jacketed column and to prevent shear-friction failure at column base. These steps, from 2 to 5, are summarized as follows.

Seismic assessment of existing columns

A developed computer code is employed to analyze an existing bridge column. The horizontal force-displacement response is generated where the shear strength of an existing column is calculated using the UCSD design model. Accordingly, the ultimate ductility capacity of the column is computed and compared with the ductility demand estimated from advanced structural analysis such as the finite element method or ductility requirement of current design guidelines. If the calculated ductility capacity exceeds the demand ductility, then no retrofit is needed. Otherwise, the following retrofit design procedure should be carried out. Full details of the seismic assessment procedure are reported elsewhere.[16]

Confinement for flexural ductility enhancement

The region of the column over which enhanced confinement should extend is designated as the plastic end region. It depends on the axial load ratio and the length of the column subjected to inelastic action. For RC bridge columns, different codes and researchers estimated the plastic end region. In this study, the criteria developed by Priestley, Seible, and Calvi[33] are followed. For axial load ratios $P/f'_{ce} A_g \leq 0.3$, the plastic end region shall be the greater of the section dimension in the direction considered and of the region over which the moment exceeds 75% of the maximum moment. For axial load ratios $P/f'_{ce} A_g > 0.3$, the plastic end region defined previously should be increased by 50%. In addition, Priestley, Seible, and Calvi[33] suggested subdividing the plastic end region into two different zones as shown in Fig. 5 for columns in single and double bending. These zones are Confinement Zone 1 at which full jacket thickness for confinement $t_{j(conf)}$, is required, and Confinement Zone 2 at which jacket thickness, for confinement, could be reduced by 50%. For flexural ductility enhancement, the required ductility capacity $\mu^{R}_{\Delta(capacity)}$ is

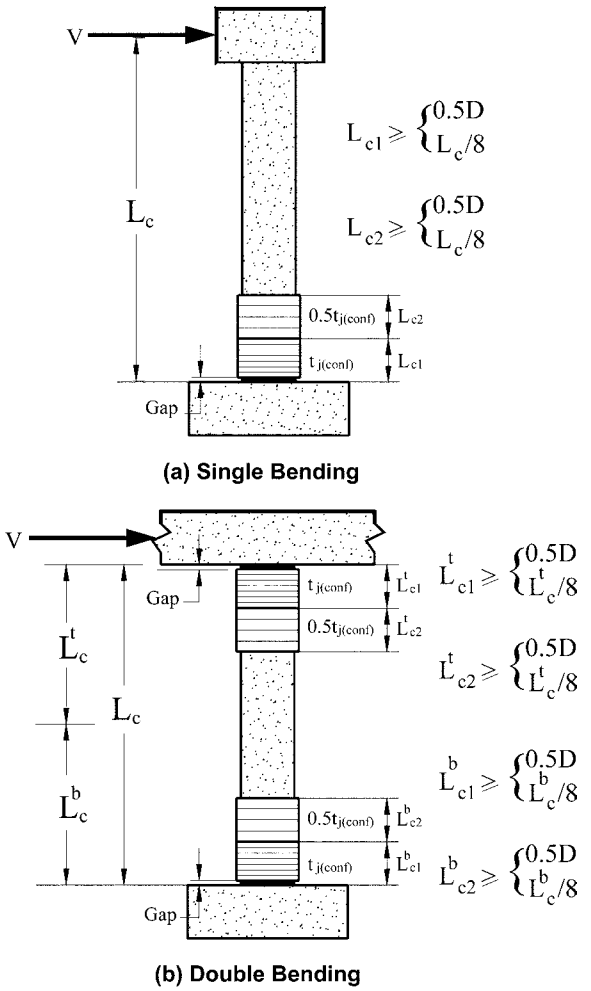

Fig. 5—Extent of fiber-reinforced polymer jacket required for plastic hinge confinement when $P/f'_{ce} A_g \leq 0.3$ *(increase by 50% when* $P/f'_{ce} A_g > 0.3$*).*

$$\mu^{R}_{\Delta(capacity)} = \frac{\mu_{\Delta(demand)}}{\varphi_{\mu}} \quad (10)$$

where $\mu_{\Delta(demand)}$ is the demand ductility and φ_{μ} is the ductility knockdown factor obtained previously in Table 8. The maximum required displacement is then determined from

$$\Delta_u = \mu^R_{\Delta(capacity)}\Delta_y \quad (11)$$

where Δ_y = idealized yield displacement for the existing column. If the plastic hinge is assumed centered at the bottom of the column to account for strain penetration into the footing, the required plastic displacement can be alternatively expressed by

$$\Delta_p = \Delta_u - \Delta_y \text{ and } \Delta_p = \theta_p L_c = \Phi_p L_p L_c \quad (12)$$

$$= (\Phi_u - \Phi_y) L_p L_c$$

where Φ_y = idealized yield curvature; L_c = clear column height; and L_p = plastic hinge length of jacketed column given by[33]

$$L_p = \begin{cases} g + 0.44 f_{ye} d_{bl} & (f_{ye} \text{ in MPa; } d_{bl} \text{ in mm}) \\ g + 0.3 f_{ye} d_{bl} & (f_{ye} \text{ in ksi; } d_{bl} \text{ in inches}) \end{cases} \quad (13)$$

where g is the gap between the jacket and the supporting member, and d_{bl} is the diameter of the longitudinal bar. The required ultimate curvature is then obtained from

$$\Phi_u = \frac{\Delta_p}{L_p L_c} + \Phi_y \quad (14)$$

The neutral axis depth at ultimate response of the retrofitted column is calculated from

$$c_{u(ret)} = k_r c_{u(existing)} \quad (15)$$

where k_r is a reduction factor estimated, for circular columns, from

$$k_r = \begin{cases} 0.90 \text{ for } 0 \le \dfrac{P}{A_g f'_{ce}} < 0.15 \\ 0.85 \text{ for } 0.15 \le \dfrac{P}{A_g f'_{ce}} < 0.30 \\ 0.80 \text{ for } 0.30 \le \dfrac{P}{A_g f'_{ce}} \end{cases} \quad (16)$$

All values of k_r for rectangular columns are smaller than those given in Eq. (16) by 0.05. The maximum required compression strain is then given by

$$\varepsilon_{cu} = \Phi_u c_{u(ret)} \quad (17)$$

The required volumetric ratio of jacket confinement ρ_j and the required jacket thickness for confinement of plastic end region $t_{j(req)}$ are given by the following equations that are based on Hosotani, Kawashima, and Hoshikuma's confinement model[3]

For circular columns—(of diameter D)

$$\rho_j = \frac{21.15 f'_{ce} (\varepsilon_{cu} - 0.00383)^{4/3}}{f_{ju(design)} \varepsilon^{2/3}_{ju(design)}} \text{ and } t_{j(req)} = \frac{D\rho_j}{4} \quad (18)$$

For rectangular columns—(of cross section dimensions b and h)

$$\rho_j = \frac{28.91 f'_{ce} (\varepsilon_{cu} - 0.00340)^{4/3}}{f_{ju(design)} \varepsilon^{2/3}_{ju(design)}} \text{ and } \quad (19)$$

$$t_{j(req)} = \frac{bh\rho_j}{2(b+h)}$$

The required number of layers is obtained by dividing the required thickness by the thickness per layer. This number should be rounded up, and a revised jacket thickness for flexural ductility enhancement $t_{j(conf)}$ is determined. The displacement ductility capacity $\mu^{calc}_{\Delta(capacity)}$ of the retrofitted column is then evaluated by the computer code, and further reduced via

$$\mu^{Red}_{\Delta(capacity)} = \mu^{calc}_{\Delta(capacity)} \varphi_\mu \quad (20)$$

to obtain the dependable ductility capacity that is compared with the ductility demand. If the design needs to be revised, the immediate previous steps are repeated assuming

$$t_{j(req)} = \frac{\mu_{\Delta(demand)}}{\mu^{Red}_{\Delta(capacity)}} t_{j(conf)} \quad (21)$$

Retrofit design for shear strength enhancement

The concrete contribution to shear strength V_c is different within and outside the plastic end region. This is considered in the UCSD shear strength model because the concrete shear strength is reduced with increased column ductility. As evidenced from experimental tests on shear-deficient columns, inclined shear cracking is anticipated at angles close to 30 degrees to the column axis, and therefore, shear cracks can be expected to extend almost twice the member depth from the critical section. Consequently, the region over which the reduced V_c component applies should be taken as $2D$ or $2h$ from the critical section for circular and rectangular columns, respectively. Within this region, a thicker jacket will be needed for shear enhancement than in regions farther from the critical section where full concrete capacity (for $\mu_\Delta \le 1$) may be assumed. It should be emphasized that jacket thicknesses calculated for shear enhancement need not be added to those required for confinement because resisting actions occur at 90 degrees to each other. Jacket configuration for shear enhancement is illustrated in Fig. 6.

For shear strength enhancement, the maximum feasible shear force of jacketed column is

$$V^o = \varphi_v V_{u\text{-}th} \quad (22)$$

where φ_v is a retrofit design factor for maximum lateral load as listed in Table 8 and $V_{u\text{-}th}$ is the maximum calculated lateral load for the retrofitted column. The demand shear force is

$$V_{demand} = \frac{V^o}{\phi_s} \quad (23)$$

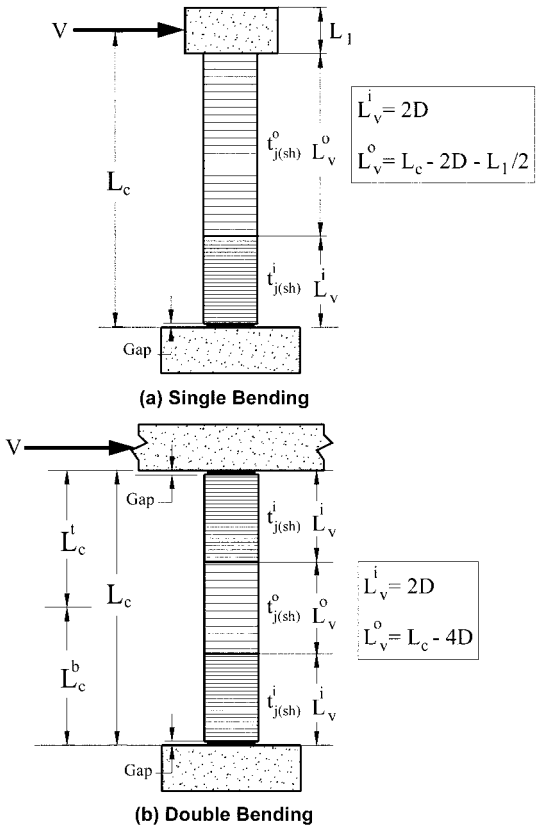

Fig. 6—Extent of fiber-reinforced polymer jacket required for shear strength enhancement.

where ϕ_s = 0.85 is the strength reduction factor recommended by ACI 318-95[13] for shear. The three components for shear resisting mechanism (V_c, V_p, and V_s) are now obtained, and the shear strength capacity of the unretrofitted column is determined from

$$V_{na} = \varphi_{sh}(V_c + V_s + V_p) \tag{24}$$

where φ_{sh} is the proposed design reduction factor for the UCSD shear model, taken equal to 0.85, as derived previously in this paper. The jacket thickness required for shear enhancement within the plastic end zone is estimated from

For circular columns,

$$t^i_{j(sh)} = \frac{159}{E_{j(design)}(D - c_{u(ret)})}(V_{demand} - V_{na}) \tag{25}$$

and for rectangular columns

$$t^i_{j(sh)} = \frac{125}{E_{j(design)}(h - c_{u(ret)})}(V_{demand} - V_{na}) \tag{26}$$

Computation of jacket thickness outside the plastic end region $t^o_{j(sh)}$ follows this same procedure except that full concrete capacity appropriate for $\mu_\Delta \le 1$ is employed. It is imperative to note that within the primary confinement zone, final jacket design will be the more stringent of $t_{j(conf)}$ and $t^i_{j(sh)}$; however, in the secondary confinement zone, the final jacket design will be the greater of $0.5t_{j(conf)}$ and $t^i_{j(sh)}$.

Limitations of jacket thickness

The designed jacket thickness determined so far should be limited to an upper bound for two reasons: 1) to avoid high shear stresses due to large lateral forces attracted by the retrofitted column during the seismic event; and 2) to avoid shear-friction failure at the base of the column.

The web reinforcement for shear strength enhancement cannot be increased indefinitely. In case of members with excessive shear reinforcement, shear failure may be brought about by web crushing caused by diagonal compression. Therefore, there is a need to limit diagonal concrete stresses to a value well below its crushing strength, that is, the shear stress level is limited to $0.2f'_{ce}$. This is assured when

$$\frac{V_{demand}}{A_e} = \frac{V^o/\phi_s}{A_e} \le 0.2f'_{ce} \tag{27}$$

where A_e is the effective shear area of the column taken as $A_e = 0.8A_g$.

To prohibit shear-friction failure at the base of seismically retrofitted columns, the following inequality should be verified

$$V_{demand} = \frac{V^o}{\phi_s} \le V_{SF} \tag{28}$$

According to Valluvan, Kreger, and Jirsa,[35] the shear-friction capacity V_{SF} can be computed from

For $P/A_g \le 5.5$ MPa (800 psi)

$$V_{SF} = \mu(P + A_s f_{ye}) \le \begin{cases} 0.25f'_{ce}\,A_g \\ 5500A_g \text{ (in kN where } A_g \text{ is in m}^2\text{)} \end{cases} \tag{29}$$

and for $P/A_g > 5.5$ MPa (800 psi)

$$V_{SF} = \mu P \le \begin{cases} 0.6f'_{ce}\,A_g \\ 14{,}450A_g \text{ (in kN where } A_g \text{ is in m}^2\text{)} \end{cases} \tag{30}$$

where μ = coefficient of friction; P = column axial load; A_s = area of longitudinal steel of the column; and f_{ye} = expected yield stress of longitudinal steel.

CONCLUSIONS

Based on a statistical analysis of experimental test data of 65 as-built circular and rectangular shear-deficient columns, it was concluded that the UCSD shear strength model provides the best correlation with all experimental data. Applying a reduction factor of 0.85 to the shear strength predicted by this model yields the appropriate design value. As for squat FRP-jacketed columns, the prediction of the seismic performance was shown to be most accurate when Wehbe's model for displacement calculation was used for circular columns and Kowalsky, Priestley and Seible's model was used for rectangular columns. Hosotani, Kawashima, and Hoshikuma's FRP-confined concrete model was proven as the most accurate for both circular and rectangular FRP-jacketed columns.

A systematic seismic retrofit methodology is further proposed based on a statistical analysis carried out on experimental database of squat FRP-jacketed columns. Because of the limited number of experimental data of such columns under lateral cyclic loading, however, the derived retrofit design factors should be recognized as guidelines only and may possibly be subject to refinement in the future with the availability of a larger database. It is also noted that the proposed retrofit design criteria are not limited to bridge columns and may be applied to RC building columns as well.

NOTATION

A_e = effective shear area of column section
A_g = gross area of column section
A_s = total area of main steel in column section
b = width of rectangular section
D = diameter of circular column
f'_{ce} = expected (most probable) concrete strength
f_{ju} = tensile strength of fiber-reinforced polymer jacket
f_{ye} = expected yield stress of reinforcing steel
h = depth of rectangular section
L_c = clear column height
L_{c1} = length of primary confinement zone
L_{c2} = length of secondary confinement zone
L_p = length of plastic hinge
L_v^i = length of shear zone within hinge region
L_v^o = length of shear zone outside hinge region
P = axial force
$t_{j(conf)}$ = thickness of fiber-reinforced polymer jacket within primary confinement zone
$t^i_{j(sh)}$ = thickness of fiber-reinforced polymer jacket for shear enhancement within plastic end region
$t^o_{j(sh)}$ = thickness of fiber-reinforced polymer jacket for shear enhancement outside plastic end region
V_{demand} = demand shear force
V_{SF} = shear-friction capacity at column base
V^o = maximum feasible shear force of jacketed column

REFERENCES

1. Mander, J. B.; Priestley, M. J. N.; and Park, R., "Theoretical Stress-Strain Model for Confined Concrete," *Journal of the Structural Division*, ASCE, V. 114, No. 8, 1988, pp. 1804-1826.

2. Samaan, M.; Mirmiran, A.; and Shahawy, M. "Model of Concrete Confined by Fiber Composites," *Journal of Structural Engineering*, ASCE, V. 124, No. 9, 1998, pp. 1025-1031.

3. Hosotani, M.; Kawashima, K.; and Hoshikuma, J.-I., "A Stress-Strain Model for Concrete Cylinders Confined by Carbon Fiber Sheets," *Report* No. TIT/EERG 98-2, Tokyo Institute of Technology, Tokyo, Japan, 1998, 55 pp. (in Japanese)

4. Hoppel, C. R.; Bogetti, T. A.; Gillespie, J. W., Jr.; Howie, I.; and Karbhari, V. M., "Analysis of a Concrete Cylinder with a Composite Hoop Wrap," *Proceedings*, 1994 ASCE Materials Engineering Conference, ASCE, New York, pp. 191-198.

5. Toutanji, H., "Stress-Strain Characteristics of Concrete Columns Externally Confined with Advanced Fiber Composite Sheets," *ACI Materials Journal*, V. 96, No. 3, May-June 1999, pp. 397-404.

6. Spoelstra, M. R., and Monti, G., "FRP-Confined Concrete Model," *Journal of Composites for Construction*, ASCE, V. 3, No. 3, 1999, pp. 143-150.

7. Kowalsky, M. J.; Priestley, M. J. N.; and Seible, F., "Shear and Flexural Behavior of Lightweight Concrete Bridge Columns in Seismic Regions," *ACI Structural Journal*, V. 96, No. 1, Jan.-Feb. 1999, pp. 136-148.

8. Wehbe, N. I.; Saiidi, M. S.; and Sanders, D. H., "Seismic Performance of Rectangular Bridge Columns with Moderate Confinement," *ACI Structural Journal*, V. 96, No. 2, Mar.-Apr. 1999, pp. 248-258.

9. Kowalsky, M. J., and Priestley, M. J. N., "Improved Analytical Model for Shear Strength of Circular Reinforced Concrete Columns in Seismic Regions," *ACI Structural Journal*, V. 97, No. 3, May-June 2000, pp. 388-396.

10. Caltrans Memo to Designers 20-4 Attachment B, *Design/Detail Guidelines*, 1996.

11. Aschheim, M.; Moehle, J. P.; and Werner, S. D., "Deformability of Concrete Columns," *Project Report* under Contract No. 59Q122, Caltrans, June 1992.

12. AIJ Structural Committee, "Design Guidelines for Earthquake Resistant Reinforced Concrete Buildings Based on Ultimate Strength Concept," Architectural Institute of Japan, 1988, 337 pp. (in Japanese)

13. ACI Committee 318, "Building Code Requirements for Structural Concrete (ACI 318-95) and Commentary (318R-95)," American Concrete Institute, Farmington Hills, Mich., 1995, 369 pp.

14. Joint ASCE-ACI Task Committee 426, "The Shear Strength of Reinforced Concrete Members," *Journal of the Structural Division*, ASCE, V. 99, No. ST6, 1973, pp. 1091-1187.

15. ATC-32, "Seismic Design Recommendations for Bridges," Applied Technology Council, Redwood City, Calif., May 1995.

16. Elsanadedy, H. M., "Seismic Performance and Analysis of Ductile Composite-Jacketed Reinforced Concrete Bridge Columns," PhD dissertation, University of California, Irvine, Calif., 2002.

17. Haroun, M. A.; Mosallam, A. S.; Feng, M. Q.; and Elsanadedy, H. M., "Experimental Investigation of Seismic Repair and Retrofit of Bridge Columns by Composite Jackets," *Proceedings of the International Conference on FRP Composites in Civil Engineering*, Hong Kong, 2001.

18. Navalpakkam, S., "Seismic Retrofit of Reinforced Concrete Bridge Columns with Shotcrete Jacket Confinement," MS thesis, University of California, Irvine, Calif., 1998.

19. Verma, R.; Priestley, M. J. N.; and Seible, F., "Assessment of Seismic Response and Steel Jacket Retrofit of Squat Circular Reinforced Concrete Bridge Columns," *Report* No. SSRP-92/05, UCSD, June 1993.

20. Priestley, M. J. N.; Seible, F.; and Benzoni, G. M., "Seismic Response of Columns with Low Longitudinal Steel Ratios," *Report* No. SSRP-94/08, UCSD, June 1994.

21. Benzoni, G.; Ohtaki, T.; Priestley, M. J. N.; and Seible, F., "Seismic Performance of Circular Reinforced Concrete Columns Under Varying Axial Load," *Report* No. SSRP-96/04, UCSD, 1996.

22. Ohtaki, T.; Benzoni, G.; and Priestley, M. J. N., "Seismic Performance of a Full Scale Bridge Column—As Built and As Repaired," *Report* No. SSRP-96/07, UCSD, 1996.

23. Ang, B. G., "Seismic Shear Strength of Circular Bridge Piers," PhD dissertation, University of Canterbury, Christchurch, New Zealand, 1985.

24. Wong, Y. L.; Paulay, T.; and Priestley, M. J. N., "Squat Circular Bridge Piers Under Multi-Directional Seismic Attack," *Report* No. 90-4, University of Canterbury, Christchurch, New Zealand, 1990.

25. Xiao, Y.; Wu, H.; and Martin, G. R., "Prefabricated Composite Jacketing of RC Columns for Enhanced Shear Strength," *Journal of Structural Engineering*, ASCE, V. 125, No. 3, 1999, pp. 255-264.

26. Iwasaki, T.; Kawashima, K.; Hagiwara, R.; Hasegawa, K.; Koyama, T.; and Yoshida, T., "Experimental Investigation on Hysteretic Behavior of Reinforced Concrete Bridge Pier Columns," *Proceedings of 2nd Joint U.S.-Japan Workshop on Performance and Strengthening of Bridge Structures and Research Needs*, San Francisco, Calif., 1985.

27. Xiao, Y.; Priestley, M. J. N.; and Seible, F., "Steel Jacket Retrofit for Enhancing Shear Strength of Short Rectangular Reinforced Concrete Columns," *Report* No. SSRP-92/07, UCSD, 1992.

28. Jirsa, J. O., and Woodward, K. A., "Behavior Classification of Short Reinforced Concrete Columns Subjected to Cyclic Deformations," *PMFSEL Report* No. 80-2, University of Texas at Austin, Austin, Tex., July 1980, 339 pp.

29. Bett, B. J.; Klingner, R. E.; and Jirsa, J. O., "Lateral Load Response of Strengthened and Repaired Reinforced Concrete Columns," *ACI Structural Journal*, V. 85, No. 5, Sept.-Oct. 1988, pp. 499-508.

30. Okamoto, T.; Tanigaki, M.; Oda, M.; and Asakura, A., "Shear Strengthening of Existing Reinforced Concrete Column by Winding with Aramid Fiber," *Proceedings of 2nd U.S.-Japan Workshop on Seismic Retrofit of Bridges*, Berkeley, Calif., 1994.

31. Seible, F.; Hegemier, G.; Priestley, M. J. N.; and Innamorato, D., "Seismic Retrofitting of Squat Circular Bridge Piers with Carbon Fiber Jackets," *Report* No. ACTT-94/04, UCSD, 1994.

32. Gallagher, D. P., "Carbon Fiber Jacket Repair and Retrofit of Reinforced Concrete Circular Bridge Columns," MS thesis, University of California, San Diego, Calif., 1998.

33. Priestley, M. J. N.; Seible, F.; and Calvi, G. M., *Seismic Design and Retrofit of Bridges*, John Wiley & Sons, Inc., New York, 1996.

34. Mirza, S. A., and MacGregor, J. G., "Variability of Mechanical Properties of Reinforcing Bars," *Journal of the Structural Division*, ASCE, V. 105, No. ST5, 1979, pp. 921-937.

35. Valluvan, R.; Kreger, M. E.; and Jirsa, J. O., "Evaluation of ACI 318-95 Shear-Friction Provisions," *ACI Structural Journal*, V. 96, No. 4, July-Aug. 1999, pp. 473-481.